A survey of non-prehensible pneumatic manipulation surfaces : principles, models and control.

Guillaume J. Laurent, Hyungpil Moon

A survey of non-prehensile pneumatic manipulation surfaces: principles, models and control

Guillaume J. Laurent* and Hyungpil Moon†

2015

Abstract

Many manipulation systems using air flow have been proposed for object handling in a non-prehensile way and without solid-to-solid contact. Potential applications include high-speed transport of fragile and clean products and high-resolution positioning of wafers. This paper discusses a comprehensive survey of state-of-the art pneumatic manipulation from the macro scale to the micro scale. The working principles and actuation methods of previously developed air-bearing surfaces, ultra-sonic bearing surfaces, air-flow manipulators, air-film manipulators, and tilted air-jet manipulators are reviewed with a particular emphasis on the modeling and the control issues. The performance of the previously developed devices was compared quantitatively.

1 Introduction

Manipulation by pneumatic medium has a long history in industrial application for conveying materials mostly on flat surfaces where grasping or touch-based manipulation should be avoided. The very original work of using air flow for conveying objects goes back a century ago to McGary's US patent 662,574 [1] which was granted in 1900 and describing an array of inclined slits through which generating tilted air-jet for material conveying. Although the patent specifies the tilted air jet supply and the side guide to form a trough, its application to handling delicate flat objects has not been issued until semi-conductor business emerges in 1970s. Wafers are handled in batch processing operations for large through-put and they are transported through a processing system by titled jets of compressed air due to the delicacy in the surface of wafers. Along with an array of inclined air-jet slits on the conveying surface, a braking function was realized with two sets of vacuum holes in [2] where one set of holes were used for braking and the other set of holes were used for relatively precise positioning. More complicated wafer multiprocessing station system in [3] requires many intersections of transporting lines to move wafers from one station to another.

*G. J. Laurent is with the FEMTO-ST Institute, UFC-ENSMM-UTBM-CNRS, Université de Franche-Comté, Besançon, France, email: guillaume.laurent@ens2m.fr

†H. Moon is with the School of Mechanical Engineering, Sungkyunkwan University, Suwon, Gyeonggi-do, Korea, email: hyungpil@skku.edu

The first attempt in modeling the air bearing (or air film in the original article) was done by Paivanas and Hassan in 1979 [4, 5, 6] where authors assumed low Reynolds viscous, incompressible, steady, and purely radial flow between plates. However, the tilted air-jet flow was not modeled analytically. Control issues such as stopping, rotating, passing through an intersection of tracks were also discussed, but only open loop control was employed. Controllable air-jet array table was firstly introduced by Konishi and Fujita in [7]. An array of controllable micro air-jet valves were fabricated on a silicon wafer using a batch-processing technique. Not only did they fabricate micro air-jet valves, but also proposed the concept of distributed manipulation using micro actuator arrays. Since then, many other types of contactless pneumatic manipulation systems are introduced such as air bearing using ultrasound [8, 9, 10, 11], manipulation using passive air flow [12, 13, 14, 15], manipulation using induced air flow [16, 17, 18, 19], manipulation using tilted air-jet array [20, 21, 22, 23, 24, 25].

Although the usage of contactless manipulation systems are dedicated to some niche markets where products can not be easily manipulated with prehensile tools such as grippers or robotic hands, air bearings are widely used in industries to transport large, thin and heavy products like glass panels. There are also relevant to handle fragile, clean, or chemically treated products. For instance, crystalline solar wafers are extremely fragile and can experience breakages brought about by the various handling technologies in the solar cell manufacturing chain. Material stress can be generated during the handling process, destroying the edges or shattering the wafer, or generating microcracks inside the wafer which are not visible to the human eye. The light weight of the wafers and their sharp edges make it difficult to consistently position the combs, which ultimately can cause wafer breakage [26]. In the semiconductor industries, low-cost thin wafer handling has also been identified as one of the difficult challenges in the 2013 International Technology Roadmap For Semiconductors Roadmap [27].

Although a noticeable technical progress has been made in the pneumatic manipulation for the last a few decades, there has been no thorough review study in the robotic community. As more demands immerse in automation of part handling in food industry, solar cell manufacturers, semi-conductor industry, and LCD industry, non-prehensile pneumatic manipulation would draw more interests from industry and also from academia. In this paper, we provide a summary of recent development of contactless pneumatic manipulation, current state of arts, merits and limitations of various air-manipulation systems, theoretical tools to analyze the phenomenon, and discuss future directions in the related research area.

The rest of the paper is organized as follows. First we discuss the issues of bearing on the bottom of the object and the manipulation flow on top of the object in Section 2. Here, we provide summaries of the theoretical analysis on the air-bearing and manipulation flow. We compare the performance of the previously developed devices as a summary. In Section 3, we discuss the modeling of exerting forces for levitation and manipulation. In Sections 4 and 5, we discuss the two major manipulation strategies, passive manipulation and active control, respectively. Passive manipulation relies on the distribution of stable equilibria of flow patterns by sequential operating flow fields. Active control manipulation makes use of visual feedback for object positioning information and uses the inverse dynamic model to find a desired set of control inputs. We conclude the article with open challenges in non-prehensile pneumatic manipulation in

Section 6.

2 Principles and devices

2.1 Air-bearing surfaces

Air bearing tables produce a cushion of air beneath the object through tiny holes like popular air hockey tables. Air bearings are widely used to transport large, thin and heavy products like glass panels [28]. Air bearing tables realize only the levitation of product, the motion is realized by another principle. For instance, gravity can be used to slide the substrates towards a direction. Conveyor belts acting on the edge of objects are widely used to index the parts in a production line. Pister *et al.* [29] demonstrated an original way of motion using electrostatic field.

Another way to produce a cushion of air is to use porous media in place of holes as proposed by Newway Air Bearings[1] and Portec[2] companies. As the porous media can be machined, this method allows to design large conveyors with very planar surface. Moreover, it produces a very homogeneous cushion of air that reduces turbulence inherent to air exhaust. Lee *et al.* [30] examined the correlation between inlet pressure, the rate of air flow, and the floating height of the glass to gain a deeper understanding of the distribution of pressure beneath the substrate and the means by which this is influenced by the permeability of porous materials. A few papers provide also some comparisons between bearings with different orifices and with porous feeding systems [31, 32]. To reduce the levitation height and to improve the stiffness of the suspension, negative pressure areas can be distributed throughout the whole surface [33].

2.2 Ultrasound bearing surfaces

Instead of pressurized air fed through orifice or porous media in aerostatic bearings, ultrasound bearings can lift a substrate over a vibrating plate (sound radiator). This levitation effect firstly reported in 1964 by Salbu [34] is known as squeeze film levitation (also called as near field acoustic levitation). The use of squeeze film levitation for production handling purposes are described for the first time the end of the 1990s [35, 9, 11, 36].

For squeeze film levitation, the levitated object must have a planar surface, and is placed extremely close (µm-range) to the vibrating surface. The pressure in the gap between the substrate and the vibrating surface rises due to the cyclic compression and decompression of the thin gas film resulting in a mean pressure $\bar{p}_r$ exceeding the ambient pressure p_0. Typical gap sizes are between 25 µm and 300 µm. Implemented industrial applications covers a large range of sizes from end effectors for wafer and parts pick-and-place to the handling of large and thin substrates such as flat panel displays, photovoltaic cells, etc. [10, 37, 8, 38] (see for example ZS-Handling products[3]). In addition to levitation, a planar object can be transported by a flexural traveling wave [39, 11]. Ueha *et al.* [11] reported

[1] Newway Air Bearings, Aston, USA, `http://www.newwayairbearings.com/`
[2] Portec, Aadorf, Switzerland, `http://www.portec.ch/`
[3] ZS-Handling, Regensburg, Germany, `http://www.zs-handling.com/`

a speed of 700 mm/s for a 90x65 mm Bakelite plate moving on a 609x70x3 mm duralumin plate excited at 19.5 kHz with vibration amplitude of 20 µm (P-P).

Ultrasound-air-bearing are usually used in conjunction with another principle to control the object position. For example, end effectors such as semiconductor wafer handlers have side stops to prevent the substrate from sliding of the gripper [9]. Micro-grippers and top-side handling systems use vacuum nozzles for self-centering and producing attraction forces [10].

2.3 Air flow manipulators

Air flow manipulation relies on two-dimensional (2D) potential flow fields on top of flat objects and air bearing on the bottom [13]. Fully developed 2D irrotational laminar flows are treated as potential flows whose velocity is proportional to the gradient of the potential and the drag force on the freely floating object is linearly proportional to the flow velocity (potential flow). A small number of point flow sinks are used for manipulation in [40] where the exerted force on a flat object is obtained from the integral of point-wise drag force due to the air flow induced by flow sinks. Quadratic flow fields can be achieved from a collection of flow sinks or continuous regions of flow sinks [14].

Instead of air sinks, flow fields can equally be induced by vertical air-jets coming out of the surface. Laurent *et al.* [16, 18, 41] used this traction principle to move a product using an array of vertical air jets to induce desired potential air flow over the surface. This device is able to move centimeter-sized objects up to 220 mm/s with millimeter closed-loop positioning accuracy.

2.4 Air-film manipulators

In 2008, Wesselingh *et al.* [42, 43] introduced a new concept of wafer positioner based on an array of cells able to generate an air film for both suspension and propulsion. The realized device consists of a 6 by 6 array of 10x10 mm cells. Each cell is supply by positively-pressurized inlets and by negatively-pressurized outlets. The pressure gradient generates an horizontal air flow that exerts a thrust force to the wafer. Moreover each cell has two inlets and two outlets placed in each corner. By varying pressure at each of the two inlet points, the flow inside the cell can be directed in two directions. The cells are etched in a thin stainless steel plate and have a depth of 10 µm. The complex flow routing to supply the cells is realized using a 3D printed manifold. The system is designed for accelerations up to 1 m/s^2 in both x and y directions for a 100 mm wafer.

First experiments were realized with low cost reflectance based optical sensors to detect the edge of the wafer. A servo error of 20 µm (P-P) and a positioning repeatability of 3 µm (STD) were reported [44]. To reduce the error, some experiments has been done in [45] with Renishaw Tonic encoders that have a resolution of 10 nm. In this case, a servo error of 0.1 µm (P-P) can be achieved. However, these sensors require that the encoding scales are etched directly on the wafer by means of laser engraving.

Suspension is achieved by setting the average pressure in the cell slightly above ambient pressure. The lower pressure at the exhaust then serves as a preload for the system, reducing the film height and increasing the stiffness of the suspension. This design is particularly interesting because, contrary to

tilted air-jet manipulators, the lifting forces and the propulsion forces can be adjusted independently. Indeed, the intensity of the thrust force is directly linked to the pressure gradient whereas the suspension height depends of the average pressure.

2.5 Tilted air-jet manipulators

The basic principle of titled air-jet manipulators relies on a set of inclined holes that create an air flow in addition to the air cushion under the object. Combination of several nozzles with different orientation can produces different functions such as transfer track, position control track, orientation control track, etc.

The main application in view is the transport and the positioning of wafers for the semiconductor industry. In the 70s, many devices have been proposed. The transporting and positioning system patented by Hagler *et al.* [2] in Texas Instruments consists of a line of tilted nozzles to lift and propel the wafers. The lateral positioning is realized by contact guides. IBM also proposed some air track systems relying on similar principles and able to transport and to position wafers in open loop [5, 4, 6, 3]. Unfortunately, none of these systems have been applied to any semiconductor manufacturing processes because of their higher running cost, their difficulties in stable transportation and positioning operations of the floating wafer, etc.

In 1997, Toda *et al.* [46, 47] improved the concept and made a transfer system for 12" wafers. The wafer track consists of a perforated plate with 0.5 mm-diameter holes intended for various functions such as floating, propelling and capturing, centering, rotating. The gas flow from these holes is controlled by a wafer-positioning sensor. Transport times of less than 15 sec, from wafer moving at 0.12 m/s to wafer stopping, were achieved in the 0.8 m-long wafer transport track. An additional suction hole is used to improved the centering of the wafer and braking the wafer motion and its speed. Positioning repeatability values of 0.18 mm in the x-direction and 0.15 mm in the y-direction are reported (without feedback).

More recently, similar systems have been investigated by Moon and Hwang [48] and by Kim and Shin [49, 50]. Kim and Shin proposed some methods to compute the precise position on the wafer with cheap photo proximity sensors but no experimental performances are reported.

In a different field, the Xerox PARK paper handling system [20, 21, 22] uses 1,152 directed air-jets in a 35 cm $\times$ 35 cm array to manipulate paper sheets. Each jet is separately controlled by an independent electrostatic zip valve. 25 linear CMOS sensor bars of 1280 pixels each are integrated between actuators to sense and control the paper position. The levitation-transport system uses two arrays of 1 mm-diameter holes tilted at 45° that are arranged in opposition to one another across a small gap in which the paper is located. The system has demonstrated closed-loop positioning repeatability in the order of 0.025 mm and trajectory tracking with typical velocity about 30 mm/s.

The system designed by Takaki *et al.* [51] is different from the conventional tilted air-jet array. They realize a variation of air jetting directions by changing the overlapped nozzle holes between two plates. The lower plate has an array of regular hole for inlet air and an array of nozzles are placed on top of it.

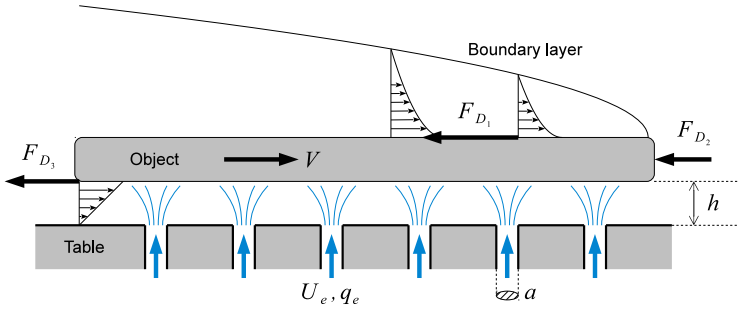

Figure 1: Principle and modeling of air-bearing surfaces.

The upper plate is translated and rotated by parallel mechanism and its motion creates the variation of air-jetting directions. The manipulated object is 20 mm by 20 mm in size and the maximum set point regulation error is about 7mm.

At a smaller scale, some tilted air-jet manipulators have been developed to move millimeter-sized object. The first device was introduced by Konishi and Fujita in 1994 [7]. An array of controllable micro air-jet valves were fabricated on a silicon wafer using a batch-processing technique. Not only did they fabricate micro air-jet valves, but also proposed the concept of distributed manipulation using micro actuator arrays.

In 1998, Hirata *et al.* [52, 53] designed a one-dimensional micro-conveyor. The fabrication combines microelectro-discharge machining and wet-etching. Maximal motion speed of 50 mm/s are demonstrated with a 3x3 mm structured silicon part. In 2006, Fukuta *et al.* [23, 24, 25] developped a new concept of MEMS-based air-jet manipulator composed of rows of controllable microactuators. The Fukuta's device is able to produce an array of tilted air-jets thanks to integrated electrostatic valves in its back side. In their experiments a flat plastic object was successfully moved with a speed of 8.3 mm/s.

Recently, Yahiaoui *et al.* [54, 55] proposed a micro-conveyor concept and its implementation. The micro-conveyor is a 9×9 mm^2 surface able to move millimeter-sized planar objects in the four cardinal directions using air flows. Thanks to a specific design, the air flow comes through a network of microchannels connected to an array of micro-nozzles. Thus, the micro-conveyor generates an array of tilted air jets that lifts and moves the object in the required direction. The micro-conveyor is able to move the object with a speed up to 137 mm/s in less than 100 ms whereas the positioning repeatability is around 0.018 mm with feedback control [56]. Numerical estimations based on an identified model shows that the speed could reach 456 mm/s if several micro-conveyors were used to form a conveying line.

The performances of the presented devices are reported in Table 1.

References	Size	Transported object	Positioning repeatability	Typical speed	Typical acceleration or force	Typical air consumption	Type of control
Toda *et al.*, 1997 [46, 47]	1000x500 mm	300 mm silicon wafer	0.18 mm (STD)	120 mm/s	120-0 mm/s deceleration in 15 s and in 800 mm	50 L/min	3-DoF (no feedback)
Hirata *et al.*, 1998 [52, 53]	20x30 mm	3x3 mm structured silicon part	Not specified	50 mm/s	0.02 mN	0.8 L/min	1-DoF motion (no feedback)
Biegelsen *et al.*, 2000 [20, 21, 22, 57]	350x350 mm	150x130 mm plastic sheet	0.025 mm (STD)	30 mm/s	0.17 mN per jet	1.2 L/min per jet	3-DoF positioning (PD feedback)
Fukuta *et al.*, 2003 [23, 24, 25]	35x35 mm	4.5x4.1 mm plastic object	Not specified	8.3 mm/s	8.3-0 mm/s deceleration in 0.215 s	Not specified	2-DoF positionning (on-off feedback)
Moon and Hwang, 2006 [48]	1000x500 mm	300 mm silicon wafer	Not specified	560 mm/s	0-560 mm/s acceleration in 300 mm	Not specified	2-DoF positioning (no feedback)
Moon, Luntz, Varsos, 2004 [15, 40, 14, 12]	300x300 mm (active area)	20x25 mm plastic object	5 mm	Not specified	Not specified	Not specified	3-DoF positionning (no feedback)
Wesselingh *et al.*, 2008 [42, 43, 44, 45]	60x60 mm	100 mm silicon wafer	0.1 µm	Not specified	1 m/s^2	Not specified	3-DoF positioning (PID feedback)
Yahiaoui *et al.*, 2010 [54, 55, 56]	9x9 mm	5 mm silicon disk	0.018 mm (ISO9283)	456 mm/s	0-137 mm/s acceleration in 0.1 s	1.8 L/min	2-DoF positionning (proportional feedback)
Delettre *et al.*, 2011 [16, 17, 18, 19]	120x120 mm	30 mm aluminium cylinder	0.1 mm	220 mm/s	20 mN	Not specified	3-DoF positioning (PD feedback, H_∞)
Takaki *et al.*, 2014 [51]	70x70 mm	20x20x10 mm	7 mm	Not specified	Not specified	Not specified	3-DoF positioning (PD feedback)

Table 1: Performances of manipulators.

3 Force Modeling

3.1 Levitation forces

A general assumption for the modeling of air-bearing tables is that the fluid is incompressible since used pressure is only several kilopascals near atmosphere. The lifting force exerted on the object can by divided in two components. The first one, the aerodynamic force, is the result of the collision of the air jet to the object back side. The momentum-flux conservation in the direction z gives:

$$F_{L_1} = k\rho q_e U_e = k\rho \frac{q_e^2}{a} \tag{1}$$

where k is the number of covered holes, ρ the fluid density, q_e the supplied gas flow rate per each hole, U_e the exit speed of gas in nozzle, a the section area of a hole.

In air-bearing tables, the aerodynamic force is usually negligible with respect to the aerostatic component. The aerostatic force is due to the distribution $p(x, y)$ of pressure beneath the substrate. This force can be calculated by integrating the pressure over the under surface S of the object:

$$F_{L_2} = \iint_S p(x, y)\ dxdy \tag{2}$$

The pressure distribution is very complex in general, especially since the air jets from the table impinge on the underside of the object at various points nonsymmetrically. Indeed, the pressure distribution depends on the location of the holes, of the flow rates, of the shape of the object and of the levitation height.

Even for simple case such as a disk centered on a single hole, an exact solution of the Navier-Stokes equation appears to be difficult. Since 1970s, a number of theoretical and experimental studies have been made [58, 59]. In 2000, McDonald proposed an approximate solution for a disk centered on a single hole assuming that the velocity is purely radial [60]. McDonald also stated a condition for this solution to be valid.

The McDonald's original equations depend on pressure differences between the center and the edge of the disk. For practical reasons, we rewrote it in terms of volumetric inflow:

$$p(r) = \frac{6\mu q_e}{\pi h^3} \ln \frac{r_d}{r} \tag{3}$$

where r_d is the radius of the disk, r the distance to the hole ($r > r_d$), μ the dynamic viscosity of air and h the levitation height.

The approximated aerostatic force is then:

$$F_{L_2} = \frac{3\mu q_e S}{\pi h^3} \tag{4}$$

where $S = \pi r_d^2$ is the surface of the disk.

This equation stands for a disk centered on a single hole on a thin air film but experiments showed that it is also a reasonable approximation for different

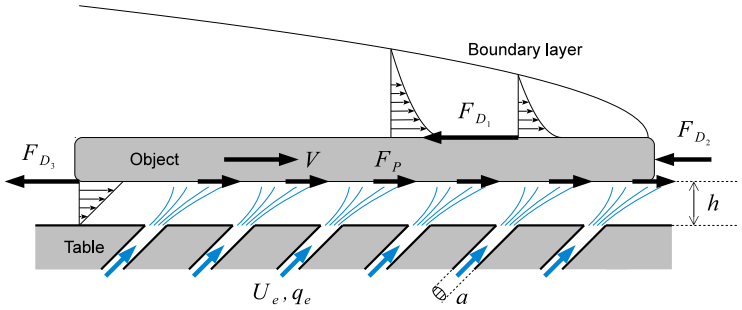

Figure 2: Principle and modeling of tilted air-jet manipulators.

shapes and multiple holes tables. In this case, q_e is simply the sum of the flow of the air jets that impinge on the underside of the object.

More precise results can be obtained using numerical integration as proposed by [31, 61].

3.2 Drag forces

When moving on the air-bearing, the substrate is slow down by the air resistance. In [46], Toda *et al.* proposed that the resistance force is the sum of the frictional resistance F_{D_1} acting on the upper surface, the drag force F_{D_2} acting on the edge, and the frictional resistance F_{D_3} acting on the underside (*cf.* Figure 1).

The frictional resistance can be calculated by :

$$F_{D_1} = \iint_0^{L(y)} \tau_w(x)\, dxdy \tag{5}$$

where $L(y)$ is the width of the upper surface for a position y normal to the direction of the displacement of the object. $\tau_w(x)$ is the local wall shear stress defined by $\tau_w(x) = 0.332V\sqrt{\frac{\rho\mu V}{x}}$ for laminar flow [62]. V is the object speed along direction X.

The drag force acting on the edge is defined by:

$$F_{D_2} = \frac{1}{2}\rho C_D A V^2 \tag{6}$$

where C_D is the drag coefficient, A the cross-sectional area of the object

The frictional resistance acting on the underside can be described by a Couette's flow and calculated by:

$$F_{D_3} = \frac{\mu S}{h} V \tag{7}$$

3.3 Forces generated by tilted air-jets

The first attempt in modeling wafer transportation systems was done by Paivanas and Hassan in 1979 [4, 5, 6]. Authors assumed low Reynolds viscous, incompressible, steady, and purely radial flow between plates to model the air bearing. However, the tilted air-jet flow was not modeled analytically.

A complete model of wafer transportation systems has been proposed later by Toda *et al.* [46]. In addition to resistance forces already presented in section 3.2, the wafer is propelled by the action of tilted air-jets (*cf.* Figure 2). The tangential force F_P exerted by a sole covered jet on the wafer can be calculated according to a drag force equation:

$$F_P = \frac{1}{2}\rho C_P a U_e^2 \sin\theta = \frac{1}{2}\rho C_P \frac{q_e^2}{a}\sin\theta \tag{8}$$

where C_P is a dimensionless coefficient and θ the inclination angle of the holes from the vertical.

In its paper, Toda did not provide any experimental validation of his model. But, Moon and Hwang [48] applied it to an air track system moving 300 mm wafers. The propulsive force coefficient C_P has been evaluated by experimental and numerical study in [63]. Depending of the flow speed, the values goes from 1.19 for $U_e = 150$ m/s to 1.45 for $U_e = 25.5$ m/s. They showed that the computed values of the speed of the wafer are larger than the experimental ones by a factor from 10% up to 47% depending of the spatial configuration of the holes.

To confirm the observation, we applied the equation 8 on the Xerox paper mover to evaluate C_P. The flow through an opened valve is given to be 0.02 L/s. Given that the diameter of the holes is 1 mm, the air speed U_e is about 25.5 m/s. Biegelsen *et al.* [21] measured the force of a jet to be 0.17 mN. Using these values, we found that C_P is about 0.78. This calculus confirms that the value found by Moon and Hwang may be overestimated.

Another problem of this model is the assumption that the force of the jet on the wafer is punctual. In fact, due to air-jet spreading, the action of the air extends beyond the wafer by several centimeters. Moreover, covered jets close to the edge of the wafer and directed to the outside direction do not transmit all their momentum before leaving the underside of the wafer.

When the object is small and does not cover many holes, this model is not appropriate. This is for example the case for micro-systems. The air flow is mainly acting on the edge of the object. Considering that an array of air-jets produces a global air flow over the surface that have a major horizontal component, Chapuis *et al.* [64] proposed to use the basic formulation of the drag force to calculate the action of the air on the object:

$$F_P = \frac{1}{2}\rho C_P A \bar{U}^2 \tag{9}$$

where $\bar{U}$ is the horizontal mean speed of the flow over the surface.

This model has been applied to the Yahiaoui's micro-conveyor in [56]. The experimental results show very good agreements with the theory. The identified values of C_D go from 0.62 to 1.27 depending of the chosen air speed. In addition, they showed that the speed of air $\bar{U}$ can be considered as proportional to the total flow rate that supplies the micro-conveyor.

3.4 Forces generated by potential air-flow

The flow patterns created by punctual air sinks are predictable using potential flow theory where the velocity field is the negative gradient of the potential [62].

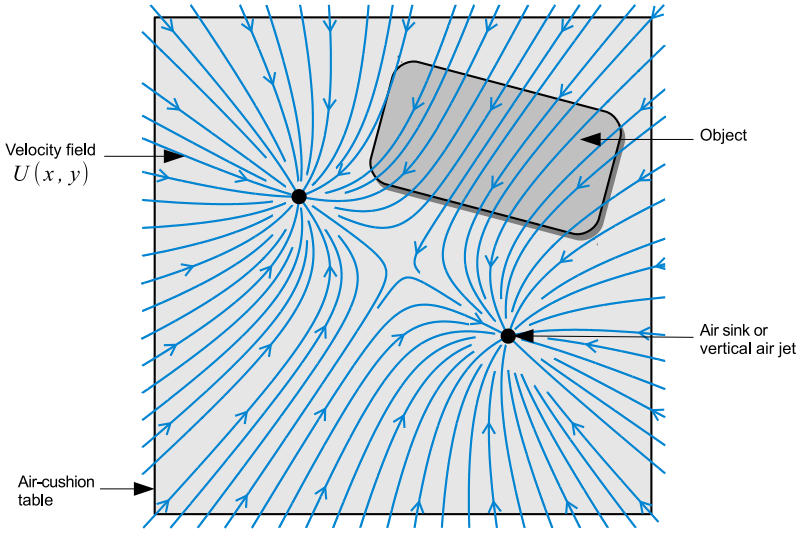

Figure 3: Principle and modeling of air-flow manipulators.

The potential function for an air sink is:

$$\phi(r, \theta) = \lambda \ln r \tag{10}$$

where (r, θ) are the polar coordinates and λ the surface flow (m^2/s). The surface flow λ is equal to q_e/h where q_e is the gas flow rate (negative for a sink) and h the air gap.

The velocity field is in the polar and cartesian forms:

$$\begin{cases} U_r &= \lambda/r \\ U_\theta &= 0 \end{cases} \quad \text{or} \quad \begin{cases} U_x &= \lambda x/(x^2+y^2) \\ U_y &= \lambda y/(x^2+y^2) \end{cases} \tag{11}$$

This velocity field is also valid for a vertical air-jet that impinges from the surface. In this case, λ is also proportional to the gas flow rate through the orifice [17].

As the floating object is manipulated in the velocity field, the total exerting force on the object is the integration of the point wise force over the surface of the object. As the integration and the derivative are both linear operation, the order of the computation is interchangeable and it creates the concept of lifted potential function (LPF) firstly introduced by Bohringer [65].

The LPF provides the net force and moment on the object.

$$F_{P_x}(q) = -\int_{D(q)} \frac{\partial u}{\partial \xi} d\xi d\eta = -\frac{\partial U}{\partial x}(q), \tag{12}$$

$$F_{P_y}(q) = -\int_{D(q)} \frac{\partial u}{\partial \eta} d\xi d\eta = -\frac{\partial U}{\partial y}(q), \tag{13}$$

$$M_P(q) = -\frac{\partial U}{\partial \theta}(q) \tag{14}$$

The net force exerting on the object in the force field is referred as lifted force. Green's theorem can further reduce the computation of the lifted force to a path integral instead of a surface integral.

$$\begin{bmatrix} F_{P_x} \\ F_{P_y} \\ M_P \end{bmatrix} = \begin{bmatrix} -\int_S u dy \\ -\int_S u dx \\ \int_s u(\vec{x} - \vec{x}_r) \cdot \vec{t} ds \end{bmatrix} = \begin{bmatrix} [\int_S u \hat{n} ds] \\ \int_S u(\vec{x} - \vec{x}_r) \cdot \vec{t} ds \end{bmatrix} \tag{15}$$

where $\hat{n}$ is the unit normal vector to the boundary of the object, $\hat{x}_r$ is an arbitrarily selected reference point on the object, and $\vec{t}$ is the unit tangential vector to the object boundary.

When the shape of the manipulating object is complex, the integration is computed numerically. In case of numeral computation, it is better to use path integral forms. The computational issues are discussed in [13]. When there are multiple flow sinks, the lifted force field can be computed from superposition of the lifted force fields for each flow sink (*cf.* Figure 3).

3.5 Summary

Regardless of the principle of propulsion (air flow, tilted air-jets, etc.), the object is subject to the sum of all the flows, air-jets and drag forces. The total forces and moment can be expressed by a linear relation to volume flows of sinks or air jets. This general formulation can be written as:

$$\begin{bmatrix} \bar{F}_{P_x} \\ \bar{F}_{P_y} \\ \bar{M}_P \end{bmatrix} = T \times \begin{bmatrix} \bar{q}_{e,1} \\ \vdots \\ \bar{q}_{e,n} \end{bmatrix} \tag{16}$$

where n is the number of sinks or air-jets and $\bar{q}_{e,i}$ is the volume flow of sinks or the square volume flow in case of titled air jets. T is the transmission matrix that coefficients depend on the principle of propulsion and on the object shape (its size is $3 \times n$).

Finally, the equation of the motion of the object is:

$$m \frac{dV}{dt} = k * \bar{F}_P - \bar{F}_D \tag{17}$$

where m is the wafer mass and $\bar{F}_D$ the sum of drag force. The same equation stands for the rotation.

The transfer functions of the dynamic part of the model is then:

$$G(s) = \frac{X(s)}{F_P(s)} = \frac{1}{ms^2 + C_F s} \tag{18}$$

where C_F is a constant that groups the coefficients of friction.

The static and dynamic parts of the model can be represented by the block diagram of Figure 4.

4 Passive manipulation

Unlike a unit radial field which is generated from a programmed actuator arrays [65], the lifted logarithmic field is not necessarily monotonically increasing when the object translates rigidly with increasing x-coordinate. Because the lifted logarithmic potential has local minima and maxima, we cannot simply

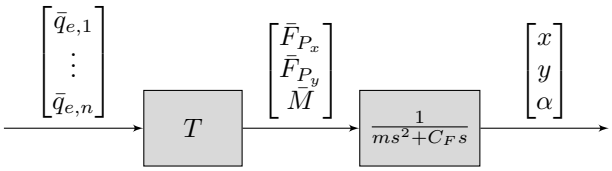

Figure 4: Synthetic model of object motion. x, y and α are respectively the position and the orientation of the object.

guarantee the uniqueness of the equilibrium in general. Also, as the flow field is conserved, in other words, the total inflow must be the same as the total outflow in a closed boundary region, the equilibria are categorized into stable ones and unstable ones. It is also important to know the stability of the equilibrium because stable ones can be used for passive air flow manipulation. For a simply connected object in a set of logarithmic radial fields, at least one sink lies on the object at stable equilibrium pose [40]. Equivalently, no stable equilibrium can exist when any simply connected object does not cover any sink.

A properly established air flow field from a small number of isolated flow sinks will manipulate an object to a predictable pose equilibrium. By sequentially applying squeeze-like flow fields, flat objects are successfully manipulated using passive air flows in [15]. The manipulating speed is very limited due to the low viscosity of air flow, but it can be improved by applying pulsing air bearing at the bottom of the floating object. The pulsing air bearing provides the air cushion only for a very short time, thus the manipulating flow induces the motion for a very short time. Such an air bearing has an effect of increasing the friction at the bottom of the object and prevents undesirable overshooting motion.

When the flow field is generated from a region of sink (not from isolated flow sinks), the net force exerting on the object becomes linear to the distance from the sink to the center of the object. Such a property is firstly introduced in [40] for a circular object and further generalized in [14] for quadratic potential force fields.

A general form of quadratic potential fields in plane is represented as follows.

$$u(\vec{p}) = \vec{p}^T \begin{bmatrix} c_{xx} & c_{xy} \\ c_{xy} & c_{yy} \end{bmatrix} \vec{p} + \begin{bmatrix} c_x & c_y \end{bmatrix} \vec{p} + c \tag{19}$$

where $\vec{p} = \begin{bmatrix} x & y \end{bmatrix}^T$ is the position vector in global coordinates. Quadratic force fields are generated from the negative gradient of the potential, therefore they are linear. Such linear force fields (Q) can be parameterized with five variables, stiffness coefficients in two directions (K_x, K_y), the orientation of the force field (ϕ_f), and the center position of the force field ($\vec{p}_0 = [x'_0 y_0]^T$). Depending on the stiffness coefficients, four types of force fields can be generated. They are elliptic field ($K_x K_y > 0$), hyperbolic field ($K_x K_y < 0$), critical field ($K_x = 0$ or $K_y = 0$), and constant field ($K_x = K_y = 0$). As elliptic force fields with positive stiffness coefficients are stable, they use them for set-point position control of an object in a passive way.

Active trajectory following can be also realizable with a sequential operation of such linear force fields by parametrizing them into translational and

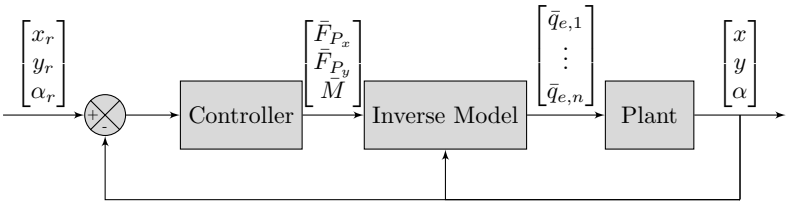

Figure 5: The inverse modeling control architecture.

centrifugal force fields. The key methodology in active superposition of linear force fields is to superimpose motion component force fields and to solve optimization problem in determining the best force field strength [12].

5 Active control of manipulation

Most of the systems use very simple on/off switches to change the rule of the device (propelling, capturing, centering, rotating). The task is then realized passively by the spatial configuration of air jets and suction points.

In the case of micro-systems, positioning tasks are usually done with intermittent air flow (or air pulse) to move the object step-by-steps [7, 66, 56]. The duration of the pulse is constant or dependent of the distance to the target position.

More advanced systems relies on closed-loop controls based on inverse modeling. The key assumption in inverse modeling control is that a plant can be made to track an input command signal when this signal is applied to a controller whose transfer function approximates the inverse of the plant's transfer function. In case of studied devices and neglecting the dynamics of the establishment of the flow, the dynamics of the object in the flow is simply a first order with integrator (*cf.* Equation 18). Thus only the inversion of the static part of the model is required.

5.1 Inverse modeling control

The usual inverse modeling architecture is depicted in Figure 5. The controller calculates the forces and moment to apply to the object according to the position errors. Then the inverse filter takes the desired forces and torque as input variables and determines the air flow rates $q_{e,i}$ of each suction point or air jet as an output variable. If the inverse model is accurate, the composite system (inverse filter + plant) is simply reduced to three independent SISO systems each one being a first order with integrator. This allows simple control designs as PD/PID to be utilized.

The problem that arises is then the solving of the linear system described by Equation 16. In general, this system is underdeterminated and has an infinite number of solutions, if any. Nevertheless not all the solutions are physically feasible. For instance, the least squares solution given by the Moore-Penrose pseudoinverse generally gives flow values $q_{e,i}$ that are too big or negative. However, this idea has been applied with success by Iwaki *et al.* [67] but with a device that have only three controlled air jets.

5.2 Static decoupling

In some specific cases, it is possible to introduce some linear dependencies between unknowns so that the system has only one solution.

This strategy has been used for example by Wesselingh *et al.* [68] to control his wafer positioner. The 36 cells of the device was supplied by 8 proportional fast piezo valves controlling the pressure. Then static decoupling of the degrees of freedom are used to calculate the pressure to be applied to the valves according to the position error.

5.3 Hierarchical force allocator

Jackson *et al.* [22, 57] used also the inverse scheme to control the Xerox paper mover. The paper sheet location and orientation are passed on to a proportional derivative controller. This controller compares the object position and orientation to a target trajectory, and computes the translational control forces and moment to be exerted on the object in order to have the object's motion match the pre-specified target trajectory. Then an actuator allocator determines the allocation for the air jets in order to produce the desired forces and torques. The role of the actuator allocator is to determine which directed jets to activate in order to provide forces that best approximate these requested forces. They propose to solve the force allocation problem as a constrained optimization problem:

$$\begin{cases} \text{minimize} & d(q_{e,1}, \ldots, q_{e,n}) \\ \text{such that} & T. \begin{bmatrix} q_{e,1} \\ \vdots \\ q_{e,n} \end{bmatrix} = \begin{bmatrix} F_{P_x} \\ F_{P_y} \\ M_P \end{bmatrix} \end{cases}$$

where the objective function d expresses the desirability of possible solutions.

For small numbers of jets, an optimal assignment of actuation can be obtained by exhaustive search, because the valves have only two states (opened or closed). If the numbers of actuators is large, Jackson *et al.* proposed to decompose into smaller subproblems using continuous solutions as approximations. It consists of grouping the jets into modules and then assigning responsibility to produce the required forces to each groups. Because of the discrete nature of the actuation, the solution is not guaranteed to be globally optimal.

Jackson *et al.* explored several possibilities of linear decomposition and found a tradeoff between the error and the computation time. Numerical simulation showed that their hybrid hierarchical-optimal algorithm work well even with thousands of actuators.

5.4 Linear programming

In order to save energy, Delettre *et al.* [17] proposed to use the total air consumption as objective function d. They also introduced some lower and upper limits to constraint the volume flow of each actuator. The previous optimization

problem becomes then a linear program:

$$\begin{cases} \text{minimize} & \sum_{i=1}^{n} q_{e,i} \\ \text{such that} & T. \begin{bmatrix} q_{e,1} \\ \vdots \\ q_{e,n} \end{bmatrix} = \begin{bmatrix} F_{P_x} \\ F_{P_y} \\ M_P \end{bmatrix} \\ \text{and} & q_{min} \leq q_{e,i} \leq q_{max} \quad \text{for} \quad 1 \leq i \leq n \end{cases}$$

The linear program consists in minimizing the linear objective function, under a set of linear constraints that have to be satisfied. A well known and efficient method for solving such a program is the simplex method.

Another advantage of this approach is that it is possible to know if there is a solution or not. This can be used to determine the maximal forces and moment that can be applied to the object by the air flow.

This general method have been validated experimentally on an air flow manipulator composed of 56 vertical air jets acting as sinks (cf. Section 2.3). At the rate of 30 Hz, three independent PID controllers evaluate the forces and moment to apply to the object according to the position errors. Then, the transmission matrix T is computed and the simplex method is ran to activate the proper air jets.

6 Discussion and Conclusion

Non-prehensile pneumatic manipulation has been used for about a century, but implementation of manipulation devices has been developed since silicon wafer processing technologies were mature. Rigorous modeling and control have been performed in relatively recent years. In this review paper, we provide theoretical levitation force modeling of air bearing and manipulation force modeling for titled air jets and potential flows. Also, we discuss the issue of open loop set-point control and feedback control using such air flows. In case of passive manipulation, analytical equilibrium conditions are useful in set-point control of an object using sequential operation of flow patterns. However, it is not so obvious what sequence of flow sinks should be placed where to have a stable trajectory following. Such a trajectory planning with linear force fields is discussed in Section 4, but no rigorous experimental verification has been performed. Active feedback control is also implementable using visual feedback of the object location and an inverse model of the air flow action.

Due to the low viscosity of the air, many devices employ the pulsed air bearing at the bottom of the floating object or the pulsed air flows for generating induced flows for manipulation. Mainly the low viscosity causes the critical limitation of pneumatic manipulation, low damping factors and bad settling time. To improve the speed of manipulation, the valve dynamics that operates the manipulation flow should be improved. Faster sensing and control law computation would increase the response time of the system. Therefore, decentralization of the sensing and control architecture would improve the speed. Some attempts have been done to decentralized the control and the sensing, notably by static decoupling and FPGA processing [66] and by reinforcement learning [69, 70]. However the problem is still largely open.

Levitation of fragile large flat objects from a solid contact surface is one of the merits of pneumatic manipulation. However, smaller parts are harder to levitate notably through the unfavourable weight/lift force ratio. It is not reported if micro size objects can be manipulated with pneumatic manipulation devices. Also, the aspect ratio of the object is an issue in levitation and manipulation. If the aspect ratio of an object is close to one, the object may not be anymore treated as a flat object. In this case, the edge effect may not be neglected. The most of devices in this review deal with two dimensional objects. Although there are literatures available about the levitation of a ball in the air based on Coanda effect [71], no device so far is reported to manipulate true three dimensional objects.

Although many previous work dream of using pneumatic manipulation in industrial applications, most of research is only to show the feasibility of the basic idea. In order to be implemented industrial applications, the performance of actuation speed and repeatability accuracy must be improved.

Nomenclature

α	object orientation
λ	surface flow
μ	dynamic viscosity of air
ρ	air density
θ	inclination angle of the nozzles from the vertical
A	cross-sectional area of the object
a	section area of a nozzle
C_D	drag coefficient
C_F	friction coefficient
C_P	propulsive force coefficient
F_D	drag force
F_L	lifting force
F_P	propulsive force
h	levitation height
M	propulsive moment
m	object mass
n	number of sinks or air-jets
p	pressure beneath the object
q_e	volume rate flowing through a nozzle

S	under surface area of the object
T	transmission matrix
U	horizontal velocity field of the flow over the surface
U_e	exit speed of air in nozzle
V	object speed along direction X
x	object position along direction X
y	object position along direction Y

Acknowledgment

This work was supported in France by the Smart Blocks project (ANR-251-2011-BS03-005), by Labex ACTION project (ANR-11-LABX-01-01) and by Région de Franche-Comté, and in Korea by the Basic Science Research Program through the National Research Foundation of Korea (NRF) funded by the Ministry of Education, Science, and Technology (2013R1A1A2013636). Hyungpil Moon was a recipient of Erasmus Mundus scholarships recommended by Prof. Nadine Le Fort-Piat at ENSMM, France.

References

[1] E. L. McGary. Air conveyer. *U.S. Patent 662,574*, 1900.

[2] R. G. Hagler. Transporting and positioning system. *U.S. Patent 3,717,381*, 1973.

[3] J. P. Babinski, B. I. Bertelsen, K. H. Raacke, V. H. Sirgo, and C. J. Townsend. Transport system for semiconductor wafer multiprocessing station system. *U.S. Patent 3,976,330*, 1976.

[4] J. A. Paivanas and J. K. Hassan. Air film system for handling semiconductor wafers. *IBM Journal of Research and Development*, 23(4):361–375, 1979.

[5] J. K. Hassan and J. A. Paivanas. Pneumatic control of the motion of objects suspended on an air film. *U.S. Patent 4,165,132*, 1979.

[6] J. K. Hassan and J. A. Paivanas. Wafer air film transportation system. *U.S. Patent 4,081,201*, 1978.

[7] S. Konishi and H. Fujita. A conveyance system using air flow based on the concept of distributed micro motion systems. *IEEE/ASME Journal of Microelectromechanical Systems*, 3(2):54–58, 1994.

[8] Michael Schilp, Josef Zimmermann, and Adolf Zitzmann. Device for non-contact transporting and holding of objects or material. *U.S. Patent 0,311,320*, 2011.

[9] G. Reinhart and J. Hoeppner. Non-contact handling using high-intensity ultrasonics. *CIRP Annals - Manufacturing Technology*, 49(1):5–8, 2000.

[10] G. Reinhart, M. Heinz, J. Stock, J. Zimmermann, M. Schilp, A. Zitzmann, and J. Hellwig. Non-contact handling and transportation for substrates and microassembly using ultrasound-air-film-technology. In *Proc. of the IEEE/SEMI Advanced Semiconductor Manufacturing Conf.*, pages 1–6, 2011.

[11] Sadayuki Ueha, Yoshiki Hashimoto, and Yoshikazu Koike. Non-contact transportation using near-field acoustic levitation. *Ultrasonics*, 38:26–32, 2000.

[12] Konstantinos Varsos and Jonathan Luntz. Superposition methods for distributed manipulation using quadratic potential force fields. *IEEE Transactions on robotics*, 22(6):1202–1215, 2006.

[13] Jonathan Luntz and Hyungpil Moon. Distributed manipulation with passive air flow. In *Proc. of the IEEE/RSJ Int. Conf. on Intelligent Robots and Systems*, pages 195–201, 2001.

[14] Konstantinos Varsos, Hyungpil Moon, and Jonathan Luntz. Generation of quadratic potential force fields from flow fields for distributed manipulation. *IEEE Transactions on robotics*, 22(1):108–118, 2006.

[15] Hyungpil Moon and Jonathan Luntz. Distributed manipulation of flat objects with two airflow sinks. *IEEE Transactions on robotics*, 22(6):1189–1201, 2006.

[16] Guillaume J. Laurent, Anne Delettre, and Nadine Le Fort-Piat. A new aerodynamic traction principe for handling products on an air cushion. *IEEE Transactions on robotics*, 27(2):379–384, 2011.

[17] Anne Delettre, Guillaume J. Laurent, Nadine Le Fort-Piat, and Christophe Varnier. 3-dof potential air flow manipulation by inverse modeling control. In *Proc. of the IEEE Int. Conf. on Automation Science and Engineering*, pages 926–931, 2012.

[18] Anne Delettre, Guillaume J. Laurent, Yassine Haddab, and Nadine Le Fort-Piat. Robust control of a planar manipulator for flexible and contactless handling. *Mechatronics*, 22(6):852–861, 2012.

[19] Anne Delettre, Guillaume J. Laurent, and Nadine Le Fort-Piat. 2-dof contactless distributed manipulation using superposition of induced air flows. In *Proc. of the IEEE/RSJ Int. Conf. on Intelligent Robots and Systems*, pages 5121–5126, 2011.

[20] Andrew Berlin, David Biegelsen, Patrick Cheung, Markus Fromherz, David Goldberg, Warren Jackson, Bryan Preas, James Reich, and Lars-Erik Swartz. Motion control of planar objects using large-area arrays of mems-like distributed manipulators. In *Micromechatronics*, 2000.

[21] David K. Biegelsen, Andrew Berlin, Patrick Cheung, Markus P.J. Fromherz, David Goldberg, Warren B. Jackson, Bryan Preas, James Reich, and Lars-Erik Swartz. Air-jet paper mover: An example of meso-scale mems. In *SPIE Int. Symposium on Micromachining and Microfabrication*, 2000.

[22] W. B. Jackson, M. P. J. Fromherz, D. K. Biegelsen, J. Reich, and D. Goldbergb. Constrained optimization based control of real time large-scale systems: Airjet object movement system. In *Proc. of the IEEE Conf. on Decision and Control*, Orlando, Florida, Dec. 4-7 2001.

[23] Y. Fukuta, Y. Mita, M. Arai, and H. Fujita. Pneumatic two-dimensional conveyance system for autonomous distributed mems. In *Proc. of the 12th Int.l Conf. on Solid-State Sensors, Actuators and Microsystems (TRANSDUCERS'03)*, volume 2, pages 1019 –1022, June 2003.

[24] Y. Fukuta, M. Yanada, A. Ino, Y. Mita, Y.-A. Chapuis, S. Konishi, and H. Fujita. Conveyor for pneumatic two-dimensional manipulation realized by arrayed mems and its control. *Journal of Robotics and Mechatronics*, 16(2):163–170, 2004.

[25] Y. Fukuta, Y.-A. Chapuis, Y. Mita, and H. Fujita. Design, fabrication and control of mems-based actuator arrays for air-flow distributed micromanipulation. *IEEE/ASME Journal of Microelectromechanical Systems*, 15(4):912–926, 2006.

[26] Leland Teschler. Next big challenge for pv makers: Wafer handling. *Machine Design*, 2008.

[27] *International Technology Roadmap For Semiconductors.* The ITRS is Jointly Sponsored by European Semiconductor Industry Association, Japan Electronics and Information Technology Industries Association, Korea Semiconductor Industry Association, Taiwan Semiconductor Industry Association, Semiconductor Industry Association, 2013.

[28] M. Hoetzle, T. Dunifon, and L. Rozevink. Glass transportation system. U.S. Patent 6,505,483, 2003.

[29] K. S. J. Pister, R. Fearing, and R. Howe. A planar air levitated electrostatic actuator system. In *Proc. of the IEEE Workshop on Micro Electro Mechanical Systems (MEMS)*, pages 67–71, Napa Valley, California, Feb. 1990.

[30] Yeeu-Chang Lee, Chin-Chang Yu, Ruey-Yih Tsai, Jen-Chung Hsiao, Ching-Hao Chen, and Sheng-Kuang Huang. Development of a porous ceramic-based air float platform for large glass substrates. *Special Topics & Reviews in Porous Media - An International Journal*, 2(4):313–321, 2011.

[31] Mohamed Fourka and Marc Bonis. Comparison between externally pressurized gas thrust bearings with different orifice and porous feeding systems. *Wear*, 210(1–2):311–317, 1997.

[32] Christoph Schenk, Stefan Buschmann, Stefan Risse, Ramona Eberhardt, and Andreas Tnnermann. Comparison between flat aerostatic gas-bearing pads with orifice and porous feedings at high-vacuum conditions. *Precision Engineering*, 32(4):319–328, 2008.

[33] Andrew J. Devitt. Non-contact porous air bearing and glass flattening device. *U.S. Patent 7,908,885*, 2011.

[34] E. Salbu. Compressible squeeze films and squeeze bearings. *Journal of Basic Engineering*, 86:355–366, 1964.

[35] Yoshiki Hashimoto, Yoshikazu Koike, and Sadayuki Ueha. Near-field acoustic levitation of planar specimens using flexural vibration. *Journal of the Acoustical Society of America*, 100(4):2057–2061, 1996.

[36] T. Amano, Y. Koike, K. Nakamura, S. Ueha, and Y. Hashimoto. A multi-transducer near field acoustic levitation system for noncontact transportation of large-sized planar objects. *Japanese Journal of Applied Physics*, 39:2982–2985, 2000.

[37] Jorgen Höppner and Josef Zimmermann. Device for contactlessly gripping and positioning components. *U.S. Patent 6,647,791*, November 2003.

[38] Josef Zimmermann, Dirk Jacob, and Adolf Zitzmann. Device for conveying and positioning of structural elements in non-contact way. *U.S. Patent 7,260,449*, August 2007.

[39] Yoshiki Hashimoto, Yoshikazu Koike, and Sadayuki Ueha. Transporting objects without contact using flexural traveling waves. *Journal of the Acoustical Society of America*, 103(6):3230–3233, 1998.

[40] Hyungpil Moon and Jonathan Luntz. Prediction of equilibria of lifted logarithmic radial potential fields. *International Journal of Robotics Research*, 23(7-8):747–762, 2004.

[41] J. Agnus, N. Chaillet, C. Clévy, S. Dembélé, M. Gauthier, Y. Haddab, G. Laurent, P. Lutz, N. Piat, K. Rabenorosoa, M. Rakotondrabe, and B. Tamadazte. Robotic microassembly and micromanipulation at femto-st. *Journal of Micro-Bio Robotics*, 2013.

[42] J. Wesselingh, R.A.J. van Ostayen, J.W. Spronck, R.H.Munnig Schmidt, and J. van Eijk. Actuator for contactless transport and positioning of large flat substrates. In *In Proc. of the EUSPEN Int. Conf.*, 2008.

[43] J. van Rij, J. Wesselingh, R. A. J. van Ostayen, J.W. Spronck, R.H. Munnig Schmidt, and J. van Eijk. Planar wafer transport and positioning on an air film using a viscous traction principle. *Tribology International*, 42:1542–1549, 2009.

[44] J. Wesselingh, J.W. Spronck, R.A.J. van Ostayen, and J. van Eijk. Contactless 6 dof planar positioning system utilizing an active air film. In *In Proc. of the EUSPEN Int. Conf.*, 2010.

[45] J. Wesselingh, J.W. Spronck, R.A.J. van Ostayen, and J. van Eijk. Air film based contactless planar positioning system with sub-micron precision. In *In Proc. of the EUSPEN Int. Conf.*, 2011.

[46] M. Toda, T. Ohmi, T. Nitta, Y. Saito, Y. Kanno, M. Umeda, M. Yagai, and H. Kidokoro. N_2 tunnel wafer transport system. *Journal of the Institute of Environmental Sciences*, 40(1):23–28, 1997.

[47] Masayuki Toda, Masaru Umeda, Yoichi Kanno, and Tadahiro Ohmi. Floating apparatus of substrate. *EP 1,005,076*, May 2000.

[48] In-Ho Moon and Young-Kyu Hwang. Evaluation of a wafer transportation speed for propulsion nozzle array on air levitation system. *Journal of Mechanical Science and Technology*, 20(9):1492–1501, 2006.

[49] Yu-Jin Kim and Dong Hun Shin. Wafer position sensing and motion control in the clean tube system. In *In Proc. of the IEEE Int. Conf. on Industrial Technology*, pages 1315–1319, 2006.

[50] D. H. Shin, H. G. Lee, and H. S. Kim. Wafer positioning control of clean tube system. In *In Proc. of the ACSE Conf.*, 2005.

[51] T. Takaki, S. Tanaka, T. Aoyama, and I. Ishii. Position/attitude control of an object by controlling a fluid field using a grid pattern air nozzle. In *Robotics and Automation (ICRA), 2014 IEEE International Conference on*, pages 6162–6167, May 2014.

[52] T. Hirata, T. Akashi, A. Bertholds, H.P. Gruber, A. Schmid, M.-A. Gretillat, O.T. Guenat, and N.F. De Rooij. A novel pneumatic actuator system realised by micro-electro-discharge machining. In *Proc of the Int. Workshop on Micro Electro Mechanical Systems*, pages 160 – 165, 1998.

[53] T. Hirata, O.T. Guenat, T. Akashi, M.-A. Gretillat, and N.-F. de Rooij. A numerical simulation on a pneumatic air table realized by micro-edm. *Journal of Microelectromechanical Systems*, 8(4):523–528, Dec 1999.

[54] Rabah Zeggari, Reda Yahiaoui, Julien Malapert, and Jean-Franois Manceau. Design and fabrication of a new two-dimensional pneumatic micro-conveyor. *Sensors & Actuators: A.Physical*, 164:125–130, 2010.

[55] Reda Yahiaoui, Rabah Zeggari, Julien Malapert, and Jean-Francois Manceau. A mems-based pneumatic micro-conveyor for planar micromanipulation. *Mechatronics*, 22(5):515–521, 2012.

[56] Guillaume J. Laurent, Anne Delettre, Rabah Zeggari, Reda Yahiaoui, Jean-Franọis Manceau, and Nadine Le Fort-Piat. Micropositioning and fast transport using a contactless micro-conveyor. *Micromachines*, 5(1):66–80, 2014.

[57] Markus P. J. Fromherz and Warren B. Jackson. Force allocation in a large-scale distributed active surface. *IEEE Trans. on Control Systems Technology*, 11(5):641–655, Sept 2003.

[58] S.D.R. Wilson. A note on laminar radial flow between parallel plates. *Applied Scientific Research*, 25(1):349–354, 1972.

[59] S.N. Dube. Linear radial flow of a viscous liquid between two parallel coaxial stationary infinite disks. *Acta Physica Academiae Scientiarum Hungaricae*, 40(2):95–103, 1976.

[60] Kirk T. McDonald. Radial viscous flow between two parallel annular plates. *arXiv:physics/0006067*, 2000.

[61] Byeong Sam Kim and Kyoungwoo Park. Numerical analysis of non contact transportation system for wafer warping. In *Proc. of the Int. Conf. on Mechanics, Fluids, Heat, Elasticity and Electromagnetic Fields*, pages 149–154, 2013.

[62] Frank M. White. *Fluid Mechanics*. McGraw-Hill Science/Engineering/Math, 2002.

[63] I.-H. Moon and Y.K. Hwang. Evaluation of a propulsion force coefficients for transportation of wafers in an air levitation system. *Korean Journal of Air-conditioning and Refrigeration Engineering*, 16(9):820–827, 2004.

[64] Y.-A. Chapuis, L. Zhou, H. Fujita, and Y. Herv. Multi-domains simulation using vhdl-ams for distributed mems in functionnal environment: Case of a 2-d air-jet micromanipulator. *Sensors and Actuators A : Physical*, 148(1):224–238, 2008.

[65] N. MacDonald K. Bohringer, B. Donald. Programmable vector fields for distributed manipulation with applications to mems actuator arrays and vibratory parts feeders. *Int. Journal of Robotics Research*, 18:168–200, 1999.

[66] Y.-A. Chapuis, L. Zhou, Y. Fukuta, Y. Mita, and H. Fujita. Fpga-based decentralized control of arrayed mems for microrobotic application. *IEEE Transactions on Industrial Electronics*, 54(4):1926–1936, 2007.

[67] S. Iwaki, H. Morimasa, T. Noritsugu, and M. Kobayashi. Contactless manipulation of an object on a plane surface using multiple air jets. In *Proc. of the IEEE Int. Conf. on Robotics and Automation*, pages 3257–3262, May 2011.

[68] J. Wesselingh, J.W. Spronck, R.A.J. van Ostayen, R.H. Munnig Schmidt, and J. van Eijk. Contactless positioning using a thin air film. In *In Proc. of the EUSPEN Int. Conf.*, 2009.

[69] Laetitia Matignon, Guillaume J. Laurent, Nadine Le Fort-Piat, and Yves-Andre Chapuis. Designing decentralized controllers for distributed-air-jet mems-based micromanipulators by reinforcement learning. *Journal of Intelligent and Robotic Systems*, 59(2):145–166, 2010.

[70] Kahina Boutoustous, Guillaume J. Laurent, Eugen Dedu, Latitia Matignon, Julien Bourgeois, and Nadine Le Fort-Piat. Distributed control architecture for smart surfaces. In *Proc. of the IEEE/RSJ Int. Conf. on Intelligent Robots and Systems*, pages 2018–2024, 2010.

[71] A. Becker, R. Sandheinrich, and T. Bretl. Automated manipulation of spherical objects in three dimensions using a gimbaled air jet. In *Proc. of the IEEE/RSJ Int. Conf. on Intelligent Robots and Systems*, pages 781–786, 2009.